We are IntechOpen,
the world's leading publisher of
Open Access books
Built by scientists, for scientists

4,800

Open access books available

122,000

International authors and editors

135M

Downloads

Our authors are among the

154

Countries delivered to

TOP 1%

most cited scientists

12.2%

Contributors from top 500 universities

CLARIVATE ANALYTICS
BOOK CITATION INDEX
INDEXED

WEB OF SCIENCE™

Selection of our books indexed in the Book Citation Index
in Web of Science™ Core Collection (BKCI)

Interested in publishing with us?
Contact book.department@intechopen.com

Numbers displayed above are based on latest data collected.
For more information visit www.intechopen.com

Current Trends in the Production of Cellulose Nanoparticles and Nanocomposites for Biomedical Applications

John Rojas, Mauricio Bedoya and Yhors Ciro

Additional information is available at the end of the chapter

Abstract

The goal of this chapter is to review the most recent trends to produce cellulose nanoparticles and nanocomposites with biomedical applications. These particles could be named as bacterial cellulose, cellulose nanofibers, and cellulose nanocrystals. The production of these nanoparticles with diameters below 100 nm is challenging because of the strong agglomeration tendency which occur upon drying aqueous cellulose suspensions or during the compounding process with hydrophobic polymers. Typically, the physical and mechanical properties of these nanoparticles depend on the source of cellulose and the extraction process employed. Cellulose nanoparticles are obtained by mechanical, chemical, or enzymatic process treatments to open the structure of the cellulose source and facilitate accessibility to its micro-structure. Usually, a combination of these processes makes the extraction more efficient.

On the other hand, cellulose and polymer nanocomposites are commonly produced by techniques such as solvent evaporation, melt compounding, compression molding, impregnation, and electrospinning. The most salient nanocellulose applications discussed in this chapter deal with the production of bandages, implants, skins replacements for burnings, face masks, artificial blood vessels, cuffs for nerve surgery, drug delivery, cell carriers, and support matrices for enzyme immobilization, and silver nanoparticles as antimicrobial agents in wound dressing.

Keywords: Cellulose nanofibers, cellulose nanocrystals, bacterial cellulose, biomedical composites

1. Introduction

Cellulose is the most abundant, renewable, and sustainable biopolymer on earth. It is present in plants, tunicates, and some bacteria. For instance, it is present in the cell wall of wood fibers along with hemicellulose and lignin. The cellulose fibers are composed of microfibrils that, in turn, are composed of elementary fibrils, which are the basic structural units. These elementary fibrils or nanofibers are about 2–20 nm in diameter and a few micrometers in length. About 30 to 100 cellulose chains aggregate into an elementary fibril. There are regions within each of these elementary fibrils, where the cellulose chains are arranged in highly ordered (crystalline) structures and regions that are disordered (amorphous) [1]. These elementary fibrils are formed during cellulose biosynthesis. Each microfibril is a flexible hair strand composed of cellulose nanocrystals (CNC) linked along with cellulose nanofibers (CNF) [2] (Fig. 1). The terms nanofibrils, nanofibers, and elementary fibrils are usually employed as synonyms. A CNF is a bulky, moderately degraded cellulose with a large surface area with diameter ranging from 20 to 60 nm and length of several micrometers. It presents a weblike structure, and the length/diameter ratio is very high. They are usually extracted by mechanical treatment without using acid hydrolysis. Conversely, when subjected to acid hydrolysis, cellulose microfibrils undergo transverse cleavage along the amorphous regions, and the use of sonication results in CNC also referred as cellulose nanowhiskers, or nanorods. Thus, CNCs are described as the crystalline region of cellulose and exhibits a rodlike shape having a low aspect ratio [2, 3]. Its elastic modulus can be compared to the modulus of crystalline cellulose (up to 140 GPa) due to its high hydrogen bonding capability. Further, cellulose nanoparticles degrade faster than other nanoparticles such as fullerenes and carbon nanotubes, which do not degrade at all [4].

Another type of nanocellulose is bacterial cellulose (BC), which is produced as an extracellular primary metabolite by bacteria belonging to the genera *Acetobacter* (*Gluconacetobacter*), *Agrobacterium*, *Acanthamoeba*, *Achromobacter*, *Zooglea*, *Aerobacter*, *Azotobacter*, *Rhizobium*, *Sarcina*, *Salmonella*, *Escherichia*, *Pseudomonas*, and *Alcaligenes* [5]. However, the most efficient producer of bacterial cellulose (BC) is *Acetobacter xylinum* (or *Gluconacetobacter xylinus*). BC is secreted as a ribbon-shaped fibril, of less than 100 nm wide, which is composed of nanofibrils of 2–4 nm in diameter. These microfibril bundles have excellent intrinsic properties due to their high crystallinity (84–89%), elastic modulus of ~78 GPa, high water holding capacity, and high degree of polymerization (up to 8,000) [6]. BC, when compressed into sheets, exhibits a highly planar orientation [7]. BC is degraded by few bacterial strains such as *Trichoderma viride* at pH values ranging from 4.5 to 6.0 [8–12]. BC is highly hydrated and no chemical treatments are needed to remove lignin and hemicellulose [13, 14]. For those reasons, BC is preferred for tissue and bone growth. The goal of this chapter is to describe and discuss the state of the art for the production of cellulose nanoparticles such as cellulose nanofibers, cellulose nanocrystals, bacterial cellulose, and their composites intended for biomedical applications.
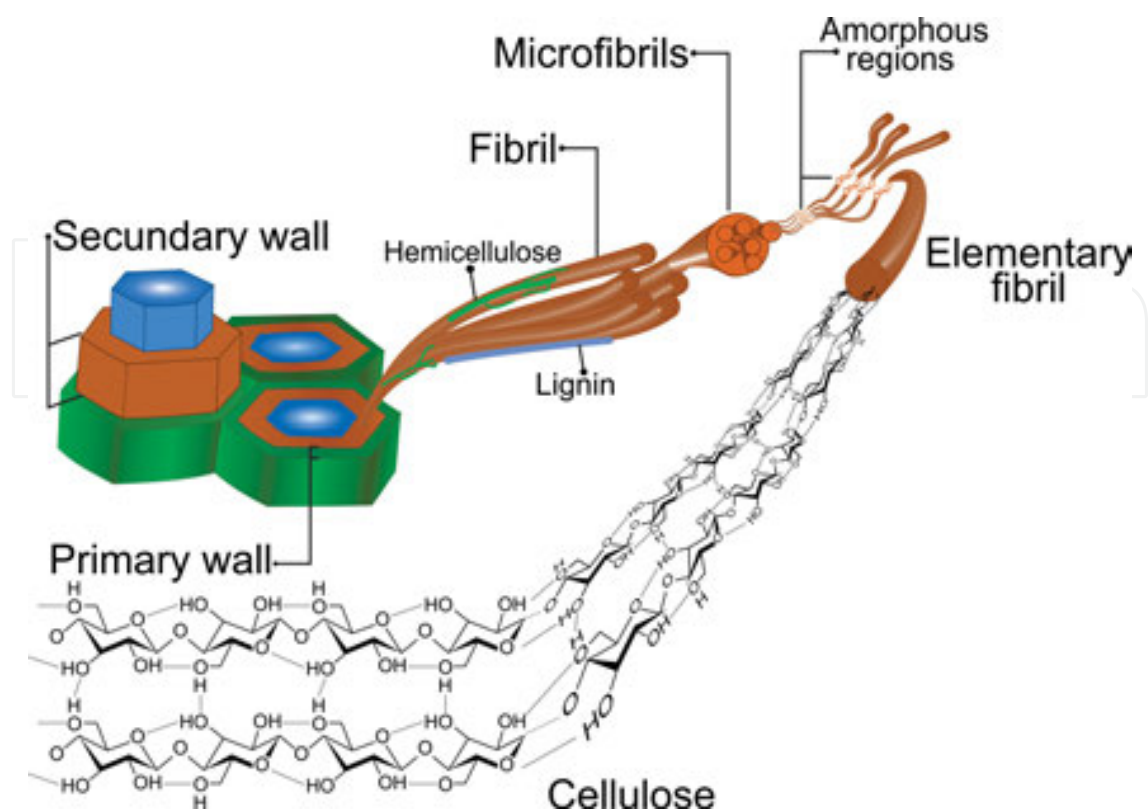
Figure 1. Hierarchical structure of cellulose extracted from plants.

2. Preparation of cellulose nanofibers

CNF is mainly extracted from wood. However, it can be extracted from natural resources such as such as sisal [15], flax, hemp, grass [16], sorghum, barley, sugar cane [17], pineapple leaf fibers [18], banana rachis [19], soy hulls [20], algae [21], bacterial cellulose, kenaf stem, swede root, wheat straw [22], carrots, empty fruit bunches, potato pulp, branch bark of mulberry [23], bagasse, rice straw, chardonnay grape skins [24], stems of cacti, coconut husk [25], bamboo, pea hull fiber, cotton and industrial bioresidues [26]. Pineapple leaf and jute fibers are the best sources for its extraction due to the low cost, abundance, and high cellulose content [60–70%) [27]. The size of CNF depends on the source and exhibits an entangled morphology with an aspect ratio over 250. For instance, CNF obtained from wheat straw, soy hull, and soybean stock have diameters ranging from 10 to 80 nm, from 20 to 120 nm, and from 50 to 100 nm, respectively [28, 29]. Nevertheless, other researchers have obtained CNF from sisal, carrots, beet pulp, and Luffa cylindrical with smaller diameters of 20–65 nm, 3–36 nm, 30–100 nm, and 55 nm, respectively. These nonwooden sources contain less lignin and require less processing steps and energy consumption due to the less tightly bound microfibril in the primary cell wall than wood. There are several extraction methods to obtain CNF [30–32] (Fig. 2). They can be performed by mechanical techniques such as grinding, cryocrushing with liquid nitrogen, high-pressure homogenization, etc. In addition, different chemical alkali and enzymatic hydrolyses can be utilized before mechanical processes in order to promote the accessibility

of hydroxyl groups, increase the inner surface, alter crystallinity, break cellulose hydrogen bonds, and therefore boost the reactivity of the fibers.

2.1. Mechanical treatments

The mechanical treatments can isolate CNF from the primary and secondary cell wall without severely degrading cellulose. For instance, microfluidization and high-intensity ultrasonic treatments produce a high shear gradients causing transverse cleavage along the longitudinal axis of the cellulose fibers, and as a result, they tend to damage the microfibril structure by reducing the molar mass and degree of crystallinity. Depending on the mechanical force levels and types of mechanical treatment, interfibrillar hydrogen bonding are broken [2, 32, 33]. However, the mechanical methods exhibit high production costs (tools and materials); they are also less efficient and require greater energy than the chemical methods [34].

For this reason, a chemical pretreatment reduces energy consumption and makes the surface more hydrophobic. Further, the mechanical treatment usually reduces the degree of polymerization (DP) from 1,200 to 1,400 to a DP between 850 and 500. A high cellulose DP is desirable since this is correlated with the nanofiber tensile strength, which can be at least 2 GPa [22, 35]

2.1.1. High-Pressure Homogenization (HPH)

In this process, dilute slurries of cellulose fibers (2–7% w/v) are passed through a spring-loaded valve assembly, at high pressure (8,000 psi), low velocity and exposed to a pressure drop to atmospheric condition while the valve opens and closes in a cyclic motion. This results in high shear and impact forces generated in a minute gap of the valve maintained at a temperature of 70–80°C [30]. As a result, the cell wall is peeled off and the DP is reduced [35, 36]. For instance, the DP is reduced from 2720 to 740 when cotton is used as a source of cellulose. Usually, this method produces fibers with diameters between 20 and 100 nm and lengths of several tens of micrometers. However, this method present some problems such as clogging of the homogenizer, high energy consumption, and mechanical damage of the crystalline microfibril structure [34, 36, 37]. HPH also decreases the crystallinity of nanofibers by increasing the number of passes.

2.1.2. Microfluidization

It is a process by which a fiber suspension is pumped through thin z-shaped chambers under a high pressure (~30,000 psi). The slurry is accelerated and led into the interaction chamber where it passes through geometrically fixed microchannels at very high velocities. Thin Z-shaped chambers with different sizes generate a high shear rate and impact forces against colliding streams. A microfluidizer generates CNFs with several micrometers in length and less than 100 nm in diameter.

2.1.3. Grinding

This is a single process by which the cellulose suspension is passed through an ultrafine grinder where the upper stone is static and the lower stone is rotating at 1400–1500 rpm. As a result, the cell wall structure is broken down by shear forces generating a gel due to the heat generated

by friction while evaporating water. However, a mechanical damage of the fiber would occur [38]. This process has been used to extract CNFs from wheat straw and soy hulls [39]. Compression is a modified grinding system by which delignified fibers of cellulosic materials are placed in a bed of stripes placed between the two plates and subjected to a constant load of 10 tons for several seconds. However, in this process fibers in the micrometer rather in the nanometer size range are obtained [40].

2.1.4. Cryocrushing

In this process, swollen cellulosic fibers are immersed in liquid nitrogen. These brittle fibers are subsequently crushed by high shear and impact forces. As a result, ice crystals exert pressure on the cell walls, causing them to rupture. Usually, this method produces CNFs with diameters ranging from 30 to 80 nm [3].

2.1.5. High-intensity ultrasonication

It is a mechanical process in which oscillating power is used to isolate CNFs by hydrodynamic forces of ultrasound [41]. During the process, cavitation leads to a formation of powerful oscillating high intensive waves. These microscopic gas bubbles expand and implode breaking down cellulose fibers. However, a large feed concentration and a large distance from probe to beaker is not advantageous for fibrillation. A typical treatment requires a cylindrical titanium alloy probe tip of 1.5 cm in diameter, high temperatures, 1000 W power, and 20–25 kHz for ~30 min [42].

2.1.6. Steam explosion

It is a thermomechanical process (200–270°C) that exposes cellulose to a high pressure of steam (14–16 bar). As a result, it penetrates the biomass by diffusion for short periods of time (20 s to 20 min), followed by a sudden decompression (explosion) generating shear forces which hydrolyze the glycosidic and hydrogen bonds between the glucose chains [31].

All the above-described mechanical methods demands a high energy consumption (20,000–30,000 kWh/tonne), which prevents their successful commercialization. Therefore, by combining the mechanical treatment with enzymatic or chemical pretreatments, it is possible to decrease the high energy consumption.

2.2. Electrospinning

In this electromechanical method, a cellulose dispersion is extruded and electrospun under the effect of a high electric field. Thus, a charged stream of cellulose dispersion is ejected following a 3D spiral trajectory. Once the solvent evaporates, it leaves behind a randomly oriented nanofibers in the collector [43]. This is a quite simple and cost-effective process. The morphology of the CNFs produced by this technology depends on factors such as the electric field strength, solution feed rate, tip-to-collector distance, etc. [43].
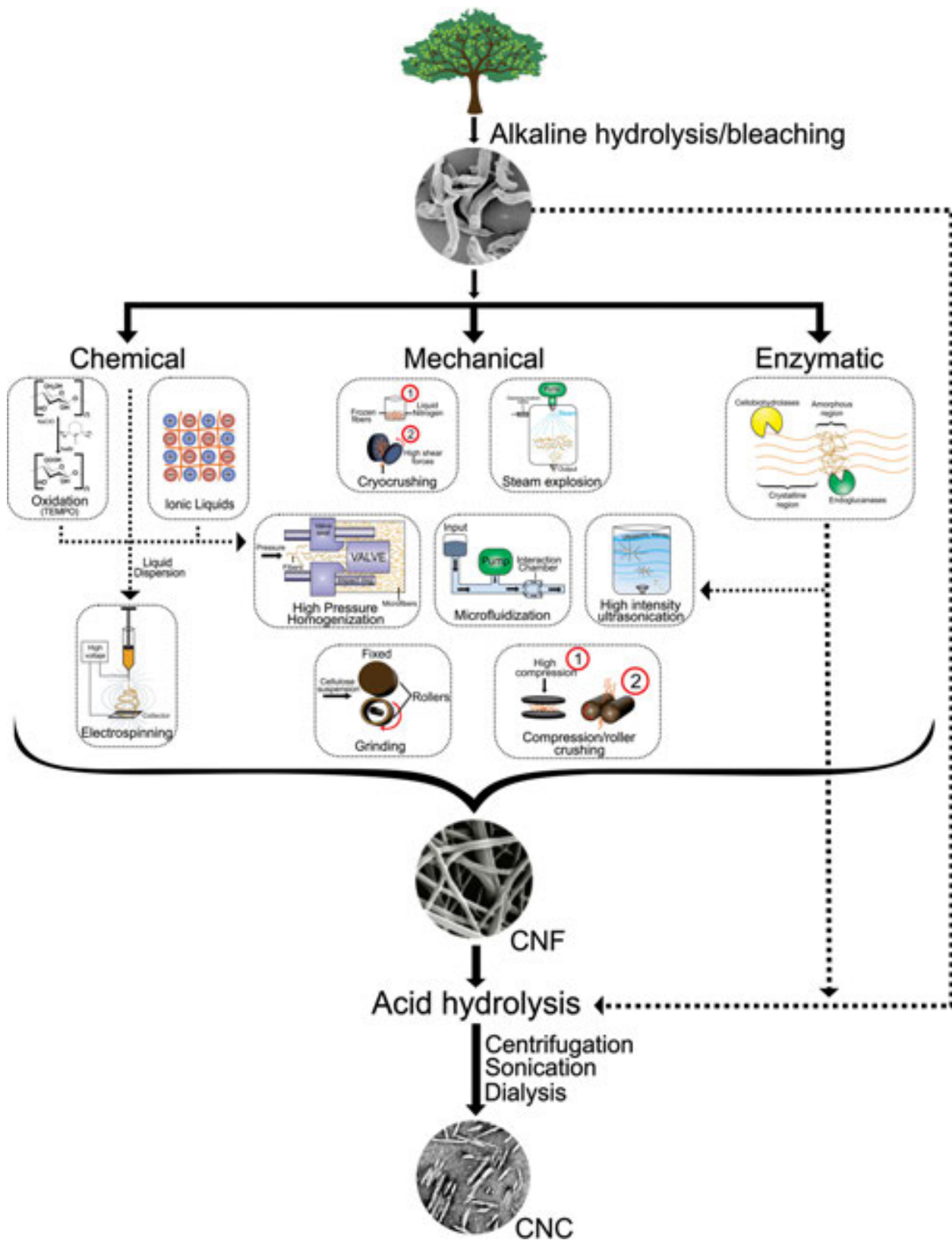
Figure 2. Conventional treatments to obtain cellulose nanoparticles.

2.3. Enzymatic hydrolysis

In this treatment, an enzyme is used to modify and/or degrade the lignin and hemicelluloses, while preventing the cellulose region. These enzymes are produced by cellobiohydrolases, which are A- and B-type cellulases able to attack the crystalline portion of cellulose, and endoglucanases C and D type, which are able to attack the disordered structure (amorphous) of cellulose [12]. Cellobiohydrolases and endoglucanases have strong synergistic effects. Thus, pretreated fibers subjected to the lowest enzyme concentration (0.02%) disintegrate, while molecular weight and fiber length are preserved. Endoglucanases cleave the noncovalent internal bonds, whereas exoglucanases attack the terminal glycosidic bonds [44]. Furthermore, *Trichoderma reesei* and *A. xylinum* produce enzymes which are able to reduce the size of microcrystalline cellulose. Enzymatic methods are highly costly due to the isolation process of the enzymes and the long enzymatic treatment time required for a successful hydrolysis [31].

3. Preparation of cellulose nanocrystals

CNCs are commonly isolated from cellulose fibers by acid hydrolysis. Tunicin is a cellulose extracted from sea animal sources made up of highly crystalline nanofibers and has an helical organization. It has a high modulus, a high aspect ratio, and good compatibility with matrix materials [45]. This cellulose is obtained by cutting into small fragments followed by bleaching. Subsequently, CNC is extracted from bleached samples by acid hydrolysis with 64 v/v% H_2SO_4, for 5 h, at 50°C. Typically, the diameter, the length, and the aspect ratio of CNC are 4–25 nm, 100–500 nm, and 15–50, respectively. Among the many cellulosic sources used for its isolation, cotton constitutes the main source. It exhibits an elongated crystalline rodlike shape and has a limited flexibility since it has no amorphous regions. These CNC have a degree of crystallinity from 55% to 90%. Moreover, the degree of crystallinity, aspect ratio, and morphology depends on the source of cellulosic material and preparation conditions [46].

A typical production process involves acid hydrolysis, washing, centrifugation, dialysis, and sonication to form a suspension followed by drying [47]. The main process for the preparation of CNCs is based on strong acid hydrolysis under strictly controlled conditions of concentration, temperature, agitation, and time. The mineral acid breaks the β-1,4 glycosidic bonds in cellulose. During hydrolysis, the amorphous regions are attacked, leaving the crystalline regions intact [48]. The resulting suspension is washed and centrifuged, and dialysis is performed to remove any free acid molecules. Microbial hydrolysis has also been utilized to produce CNCs. This microbial hydrolysis is eco-friendly and does not require any surface modification [44]. The charge and colloidal behavior of CNCs depends on the acid used for the production. Sulfuric and hydrochloric acids are the most commonly used, but phosphoric and hydrobromic acids have also been used [7].

For instance, hydrolysis with 63.5 v/v% H_2SO_4 for 2 h leads to a 30% yield, a width narrower than 10 nm and length ranging between 200 and 400 nm [3]. Smaller CNCs are obtained by increasing hydrolysis time and acid concentration [15]. Another treatment employs wood pulp

boiled with 2.5 N sulfuric acid for 12 h, generating CNCs with lengths between 50 and 60 nm and widths between 5 and 10 nm [49].

The physical characteristics of CNCs depend on the origin of cellulose sources, concentration of acid, types of acid, reaction time, and temperature [3]. If sulfuric acid (50–70% w/v), temperature of 20–70°C, rate of 500 rpm, and time of 0.5–6 h are employed, esterification also occurs forming "cellulose sulfate," resulting in a negatively charged surface on the cellulose crystallites. Longer hydrolysis time and higher temperature generate shorter nanocrystals with higher surface charge, high crystallinity (~80%), and narrower polydispersity [50–53]. However, the very limited commercial availability of CNC is due to the time consuming production process and the low yield produced, especially if the initial amount of amorphous cellulose is very high. The aggregation of CNC occurs with HCl, but sulfuric acid creates charged sulfate esters promoting the dispersion of the CNCs in water preventing aggregation. The combination of both sulfuric and hydrochloric acids during hydrolysis generates spherical nanoparticles with improved thermal stability due to the reduced presence of sulfate groups on their surface. The negative surface charge of CNCs stabilizes the aqueous suspension against flocculation, but this charge also compromises the thermostability of nanocrystals. Therefore, the increase in the sulfate group content decreases the temperature at which thermal degradation takes place [54]. CNCs also exhibit chiral nematic liquid crystalline alignments, which are seen as a flow of birefringence between two crossed polarizing films.

4. Pretreatment processes

The aim of the pretreatment process is to remove ashes, waxes, lignin, hemicellulose, and other noncellulosic compounds, which are crucial to produce pure cellulosic products such as CNFs and CNCs [30–32]. A pretreatment also reduces the energy demand of mechanical processes from 20,000 to 30,000 kWh/tonne to 1000 kWh/tonne. The types of pretreatments applied on different raw materials such as tunicate, algae, and bacteria cellulose have been reported previously [21, 55]. The alkaline delignification and organosolvation with acetic acid, aqueous methanol, or ethanol are also considered as pretreatment processes [56, 57].

4.1. Alkaline hydrolysis

Alkaline treatments are conducted when a more effective lignin, hemicellulose, and pectin solubilization and removal is needed. Alkaline extraction needs to be controlled to avoid cellulose degradation [3]. A typical treatment involves dipping of fibers in a 5% sodium hydroxide solution for ~48 h at 30°C. At pH >12, NaOH reduces super oxide radicals (-O$_2$), wherein lignin and hemicellulose are hydrolyzed [15]. However, if lignin content is high in the cellulosic source, the nanocellulose yield is low [15, 58].

4.2. Bleaching

Pulp can be bleached to improve ageing resistance avoiding yellowing and brittleness. These two defects are mainly related to the presence of lignin. Different compounds are commonly

used for bleaching. These include hydrogen peroxide (H_2O_2), chlorine dioxide (ClO_2), ozone (O_3), peracetic acid, and $NaClO_2$. Sulfite pulps are more readily bleached and results in high yields [59].

4.3. Oxidation

The TEMPO-mediated surface oxidation is the most commonly used chemical pretreatment conducted under aqueous and mild conditions. It converts the primary hydroxyl group (C6) to a charged aldehyde or carboxylate functional group, whereas the secondary hydroxyl moieties present in the cellulose molecule remain unaffected [1, 12]. The oxidation of cellulose fibers occurs in the presence of NaClO and catalytic amounts of 2,2,6,6 tetramethyl-1 piperi-dinyloxy radical (TEMPO) and NaBr as catalyst at a pH between 9 and 11 and room temperature. The higher the amount of NaClO in the reaction medium, the larger is the number of carboxylic groups formed at the surface of the CNFs and the stronger is the decrease in DP [44]. This oxidation creates negative charges on the surface of CNC [31] without changing the original fibrous morphologies [61–66]. The reaction by-product is only sodium chloride. Other N-oxyl compounds, such as the 4-hydroxy TEMPO derivative (less expensive than TEMPO), have been proposed. The residual aldehyde groups causes discoloration. In order to avoid depolymerization or discoloration of the oxidized cellulose, a TEMPO/NaClO/$NaClO_2$ system is employed under neutral or slightly acidic conditions [60]. This treatment also prevents the postaggregation of nanoparticles during the drying step.

A variation of this condition oxidizes wood cellulose rendering CNF with a higher molecular weight and with no aldehyde groups using a TEMPO/NaClO/$NaClO_2$ system at pHs ranging from 5 to 7 [67]. The TEMPO pretreatment eases the separation of the nanofibrils from each other due to the repulsive forces of the ionized carboxylate groups, which overwhelm the hydrogen bonds. The TEMPO oxidation pretreatment is usually followed by a mechanical treatment. Other less commonly used processes include oxidation at 60°C with ammonium persulfate and the sequential periodate and chlorite oxidation [68].

4.4. Ionic liquids

Ionic liquids are organic salts having no corrosive properties, no flammability, a melting point below 100°C, low vapor pressure, and low viscosities [34]. Ionic liquids dissolve cellulose and render a wide range of particle morphologies after precipitation. The ionic liquid breaks intramolecular hydrogen bonds, whereas the cations attack the O atom of the –OH, and anions attack the hydrogen atoms of the -OH group [34]. PF_6^-, BF_4^-, $(CF_3CO_2)^-$, $(SbF_6)^-$, $(OTS)^-$, $(ClO_4)^-$, $(GeCl_3)^-$, $(Al_2Cl_7)^-$, and $(AlCl_4)^-$ are the most common anions employed [69, 70].

5. Nanocellulose derivatization

This chemical treatment is performed on the surface of BC, CNC, or CNF for making them more hydrophobic reducing the agglomeration tendency of these materials. The goal of the

derivatization is to endow nanocellulose with a hydrophobic character in order to improve its compatibility with nonpolar polymers [60, 71–73].

5.1. Carboxymethylation

This process makes the surface negatively charged, promotes the formation of a stable suspension, and increases the breakup of lignocellulosic fibers [2]. If carboxymethylation is conducted before mechanical treatment, the fibers become more dispersible having a lower degree of crystallinity [72].

5.2. Acetylation

In this reaction, the C6 hydroxyl groups of cellulose are selectively converted to carboxylate groups and only NaClO and NaOH are consumed. The amount of carboxylate groups formed increases with the amount of NaClO and by employing long reaction times [74]. This reaction causes plasticization of lignocellulosic fibers [31] [54]. Further, a reaction of CNF with acetic anhydride at 105°C for 30 min causes a degree of substitution (DS) of 0.43. As a result, the contact angle increases from 33° for nonacetylated nanofibers to 115° for acetylated ones. The acetylated fibers have a lower crystallinity due to degradation of crystalline regions during the reaction.

5.3. Isocyanate

Isocyanates, in particular, octadecyl isocyanate, can generate covalent bonds with hydroxyl groups on the particle surface, rendering a degree of substitution of 0.07 and 0.09 for CNC and NFC, respectively [75].

5.4. Silylation

The reaction between silanol and OH groups of cellulose at high temperature is initiated by water. Surface silylation of CNFs from bleached softwood pulp using chlorodimethyl isopropylsilane renders a degree of surface substitution from 0.6 to 1. Conversely, silylation of CNFs by isopropyl dimethylchlorosilane renders a CNF that forms suspensions with a shear-thinning behavior [54].

6. Physical properties

6.1. Morphology

Depending upon the source of the cellulose and the method of production, a CNF displays similar morphologies but several dimensions. Typically, a CNF and a CNC have typical diameters of 2–100 nm and between 2 and 30 nm, respectively. For instance, CNFs from wheat straw have diameters from 10 to 80 nm [22] as compared to soy hulls (20–120 nm) [20], kenaf bast (2–6 nm), wood (15 nm), bagasse (5–15 nm), rice straw (4–13 nm), soybean stock-based (50–100 nm), cotton (10– 25 nm), and empty fruit bunch (10–30 nm) [31, 76–85].

6.2. Crystallinity

Crystallinity is highly dependent on the lignocellulosic source. For instance, crystallinity of flax, rutabaga, and wood CNFs are 59%, 64%, and 54%, respectively, whereas a crystallinity of 85.9%, 76%, 84.9%, 94%, 80.6%, and 81.7% has been found for CNCs obtained from sisal, rice husk, flax, cotton, corn stover, and commercial MCC, respectively. On the other hand, a DC of 78% and 70% has been obtained for wheat straw [22] and soy hull CNFs, respectively. Further, very low values have been obtained for beet pulp ~30–40% [20]. The degree of crystallinity ranges in the order: pineapple > banana > jute, and this order agrees with the values of cellulose content determined in these samples. Usually, CNCs prepared from H_2SO_4 have lower crystalline values than those prepared from HCl. In addition, the increase in hydrolysis time also increases crystallinity due to the elimination of amorphous regions [15].

6.3. Thermal properties

The thermal degradation of lignocellulosic materials begins with an early decomposition of hemicelluloses, followed by an early stage of pyrolysis of lignin, depolymerization, active flaming combustion, and char oxidation. Further, CNF has a high degradation temperature onset (350°C) and better thermal behavior than hemicellulose, pectin, and lignin. On the contrary, the onset of the thermal degradation of CNC typically occurs at 200–300°C[86]. CNC with lower sulfate content have better thermal stability [53]. On the other hand, banana CNF exhibited three main weight loss regions. The initial weight is mainly due to moisture evaporation followed by thermal depolymerization of hemicellulose and the cleavage of glycosidic linkages of cellulose. The broad peak in the region from 200°C to 500°C is due to residual lignin components. A convection drying of a CNF removes water slowly causing the formation of aggregates. Therefore, the dried CNF presents a lower degree of thermal stability than that of the original fibers. [19].

6.4. Degree of Polymerization (DP) and mechanical properties

DP is strongly correlated with the aspect ratio of the nanofibers. As explained previously, any pretreatment process also reduces the DP. On the other hand, the mechanical properties of cellulose nanoparticles depend on morphology, geometrical dimensions, crystal structure, crystallinity, and the process used to produce CNCs and CNFs. For instance, the DP of softwood is 2249, but the DP of sulfated CNF is 825. Further, the tensile strength of native CNCs ranges from 7.5 to 7.7 GPa. Further, the Young's modulus of CNCs is estimated to lie between 130 and 250 GPa.

6.5. Hornification

Drying of individual cellulose nanoparticles creates irreversible agglomeration affecting their dimension and, therefore, their unique properties [87]. This irreversible agglomeration is known as hornification and is related to the hydrogen bonds formed [81]. If freeze-drying or supercritical dying with CO_2 is used, agglomeration is avoided [87–89].

6.6. Film properties

CNF gels can be diluted and either cast or vacuum filtered followed by drying to form stiff films due to the formation of an interfibrillar hydrogen bonding network [63, 90–93]. For instance, CNF films obtained from sugar beet have values of tensile strength and modulus of 104 MPa and 3.5 GPa, respectively [37, 61, 94].

6.7. Surface area

Cellulose nanoparticles have a high specific surface area (SSA). Typically, cellulose nanoparticles have SSA ranging from 50 to 200 g/m^2. Conversely, the SSA of nanocellulose aerogels ranges higher from 250 to 350 m^2/g and have a very low density (0.02 g/cm^3) and a high porosity of 98% [61, 63, 94].

6.8. Rheological properties

CNF suspensions exhibit a shear-thinning behavior and pseudoplasticity, which in turn depends on the pH medium [95]. Further, sulfate cellulose shows a pH-dependent viscosity profile due to electrostatic interactions. Moreover, a CNF suspension has a decreasing viscosity with increasing shear rates. Further, CNF also has a high elastic modulus due to the entangled network structure [96].

6.9. Water sorption and permeability

CNFs are able to form films with a low moisture diffusivity due to a rigid fiber network [90] and, thus, have excellent barrier properties [90]. The water vapor transfer rate (WVTR) of CNFs films are 20% smaller than those made of macrofibers (from 20% to 30%). CNC films are expected to provide a better barrier to water since CNC films have a more crystalline nature than CNF [90].

6.10. Oxygen barrier

The oxygen transmittance rate of CNF at 0% RH is in the range 17–18 $mL/m^2/day$. The increase of RH increases the oxygen permeability due to the limited hydrogen bonding and loose network caused by the incoming water molecules. The water and oxygen permeability decreased with increasing film thickness due to the lack of interconnectivity of pores [63].

7. Toxicity

CNCs have low toxicity and low environmental risk according to ecotoxicological tests with several aquatic species (e.g., Daphnia, rainbow trout and fathead minnow). Further, cytotoxicity (intracellular toxic effect) and proinflammatory response are significantly lower than those for MWCNT (multiwalled carbon nanotubes) and CAF (crocidolite asbestos fibers). CNF shows no toxicity and genotoxicity in vitro [97]. The toxicity of BC nanofibers has been

successfully evaluated in vitro through cell viability and flow cytometric assays and in vivo using C57/B16 mice surgeries. Further, BC shows no toxicity in human umbilical vein endothelial cell culture, fibroblasts, and chondrocytes. The in vitro evaluation also shows that 95% of the mesenchymal stem cells aggregate to cellulose membrane [98, 99] (Fig. 3).
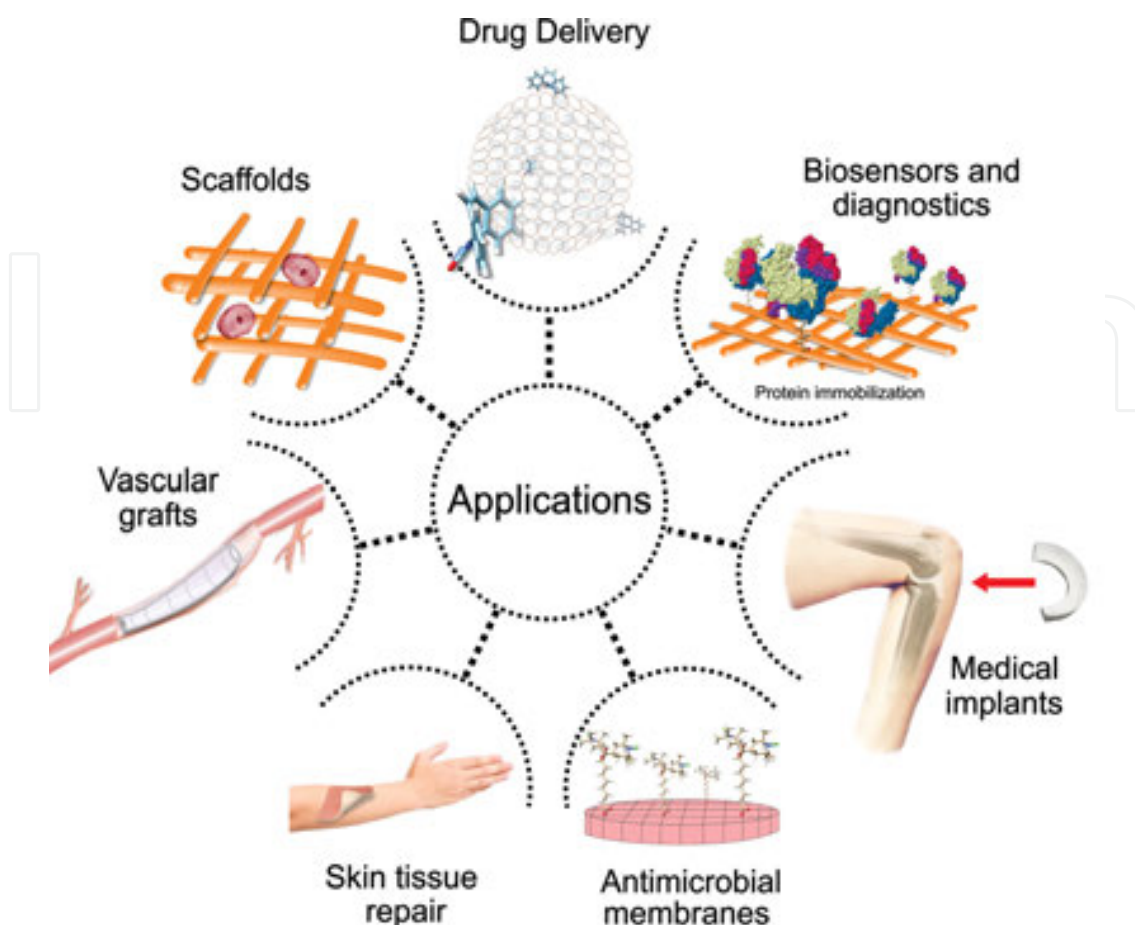
8. Biomedical applications

8.1. Biological benefits

Nanocellulose has been mainly used as a filler in nanocomposites because of its good mechanical properties due to their biodegradability, renewability, availability, sustainability, lower cost, lower weight, higher mechanical strength, biocompatibility, high hydrophilicity, and high surface area [94, 100, 101–105]. It evades adverse tissue reactions, and unlike proteins, its polysaccharide nature makes it less immunogenic and nonhemolytic. It also promotes cellular interaction and tissue development. It is a slow/nondegrading material in vivo and in vitro, which makes it suitable for use as a scaffold providing a long-term support, sustains high loads, and has a high wear resistance. The biomedical industry includes skin replacements for burnings and wounds; drug releasing system; blood vessel growth; nerves, gum, and dura mater reconstruction; scaffolds for tissue engineering; stent covering; and bone reconstruction. The cellulose nanoparticle surface dictates cellular response by interfering with cellular adhesion, proliferation, migration, and functioning. On the other hand, cells support, hold, synthesize the matrix for the new tissues, and keep the proper growth ambient, whereas the growth factors promote the cell regeneration [97, 101, 106, 107].

In one study, a charged CNC–FITC and newly synthesized CNC–rhodamine B isothiocyanate (RBITC) were synthesized, and in vitro cellular uptake studies showed that the positively charged CNC-RBITC was taken up by human embryonic kidney (HEK) and *Spodoptera frugiperda* (Sf9) cells without any noticeable cytotoxic effect on the two cell lines [108].

8.2. Biosensors and diagnostics

CNFs serve as a suitable platform for immobilization of bioactive molecules (e.g., enzymes, antibodies, etc.), which is useful in biosensors and diagnostics. For example, novel gold bacterial cellulose (Au-BC) nanocomposites have been prepared by a one-step biotemplated method in aqueous suspensions. This material shows excellent biocompatibility, good conductivity, and ultrafine nanofiber network structure, which makes it able to entrap horseradish peroxidase (HRP), maintaining enzyme bioactivity. HRP biosensors allow detection of H_2O_2 with a detection limit lower than 1 μM [109]. CNF films carboxlylated with TEMPO and activated via EDC/NHS coupling have been used to immobilize the antibody (antihuman immunoglobulin G (anti-IgG)) by physical adsorption. This surface can detect positively charged molecules. A TEMPO-activated film has also been used to conjugate Avidin for selectively capturing biotinylated molecules (anti-IgG) [109, 110].

Figure 3. Biomedical applications of cellulose nanoparticles.

Another study showed CNF to prepare support films with carboxyl groups, which are then converted to amine-reactive species. These substrates were then used to bind polyclonal anti-IgG. The CNF surface can also be activated by copolymer grafting. Thus, a peptide with specific affinity to human IgG is conjugated to the grafted polymer having a high selectivity.

Proteins such as collagen, elastin, hyaluronan, and growth factors such as the basic fibroblast growth factor (B-FGF), human epidermal growth factor (H-EGF), and keratinocyte growth factor (KGF) have been immobilized on macroporous BC to improve biocompatibility. The attachment of cells can be improved by utilizing adhesive amino acid sequences, such as Arg-Gly-Asp (RGD) found in several extracellular matrix proteins [111, 112].

Peptides such as the HWRGWV peptide can be immobilized on the TEMPO-activated film to detect human IgG. Thus, the acetylated peptide is covalently immobilized to the spacers on CNF via amide reaction. For instance, chitosan can be physically adsorbed onto the CNF and used as a spacer. The resulting biosensor has a very high specific binding capability for IgG and exhibits excellent resistance for nonspecific protein adsorption [113]. In another study, Edwards et al. created biosensors based on CNC by peptide conjugation for detection of human neutrophil elastase [114].

On the other hand, CNCs have been used as electrochemical sensors to selectively detect DNA hybridization. DNA oligomers were grafted onto TEMPO-oxidized CNC produced from cotton. This DNA-grafted CNC is able to self-assembling into larger aggregates as compared to the unmodified CNC. In another study, silver nanoparticles were obtained onto TEMPO-mediated oxidized CNC by using $NaBH_4$ as a reducing agent. The presence of CNC prevented the aggregation of the nanoparticles [115].

Moreover, the layer by layer (LbL) assembly technique has been used to adsorb collagen onto the surface of CNF. The LbL technique has also been used to prepare a luminescent single-walled carbon nanotube–CNC films enhancing their water dispersibility [116].

Dong et al. synthesized folic acid (FA)-grafted CNCs and explored their folate-receptor-mediated uptake by human and rat brain tumor cells. First, CNCs were labeled with fluorescein isothiocyanate (FITC) for detection in the cells and were then conjugated with FA. In vitro studies showed that the cellular binding of the FITC–CNC–FA by the folate receptor (which is overexpressed by cancer cells) was higher than that of the free FA [117].

8.3. Skin tissue repair

Nanocellulose membranes could serve as an infection barrier, prevent loss of fluids, have a painkiller effect, allow drugs to be easily applied, and also absorb the purulent fluids during all inflammatory stages, expelling them later on in a controlled and painless manner [118].

Properties such as biocompatibility, high superficial area, high water absorption capacity, high elastic modulus, low thermal expansion coefficient, optical transparency, anisotropy, and flexible surface chemistry endow nanocellulose with suitable wound dressing applications. For instance, a membrane has been developed with BC and propolis extract, rendering antimicrobial and anti-inflammatory activities in chronic wounds absorbing purulent exudates. Further, it eases the BC removal from a wound surface after recovery [97].

Traditionally, skin tissue repair materials have been absorbent, permeable materials such as gauze, which can adhere to desiccated wound surfaces inducing trauma upon removal [119, 120]. BC controls wound dressing since it can control wound exudates and can provide a moist environment to a wound resulting in better wound healing. For instance, Biofill® is a commercial product of BC used as a temporary substitute for human skin in cases of second and third degree burns.

Czaja et al. showed that the skin of the patients whose burns were covered with a BC membrane healed faster than the wounds of patients who received conventional wound dressings. This is explained by the faster tissue regeneration, capillary formation and cell proliferation [121].

In a different study, BC wound dressing materials were compared to two different commercial dressings, Vaseline gauze, and Algisite M in a rat model. This study showed that BC-dressed animals had more rapid wound healing within 14 days without any evidence of toxicity [122]. Further, BC, gelatin, and alginate composite membranes showed the successful growth of NIH/3T3-type cells and, hence, proved potential as a skin tissue regeneration template [123].

The addition of chitosan to a tempo-oxidized BC renders a composite with high superior mechanical properties, water holding capacity, and water release rate, and thus, these composites can be used for wound dressing [124].

BC has also been used in a surgery of the lateral wall of the nose preventing nasal bleeding, surgical wound infections, local pain, and clotting [125]. Therefore, it provides a more rapid healing without the formation of crusts and prevent infection without the need for removal as compared to commercial nasal packing which causes a great discomfort upon removal [125].

A nanocellulose membrane has also been implanted into the subcutaneous tissue of diabetic rats for 12 weeks. Rats showed no macroscopic signs of inflammation around the implants, no formation of fibrotic capsule or giant cells, and fibroblasts were fully integrated to the cellulosic membrane and started to synthesize collagen [126].

8.4. Cortical implants

Neural interfaces are able to record neural signals from individual neurons or small groups of neurons in the brain. The most common neural interfaces are made of iridium oxide, silicon, platinum, titanium, glassy carbon, gold, and stainless steel. However, they cause glia encapsulation at the electrode interface, leading to neuron death near the surface of the implanted electrode. For this reason, adaptive cellulose nanoparticles interfaces should be stiff enough to be easily implanted into the brain but subsequently soften under in vivo conditions to closely match the stiffness of the brain tissue.

This nanocellulosic interface relies on stiff collagen fibers dispersed throughout a soft fibrillin matrix. Because of the abundance of surface hydroxyl groups, CNCs strongly interact with each other through hydrogen bonding and/or van der Waals' forces, but exposure to water reduces CNC–CNC interactions because of competitive hydrogen bonding or interfacial interactions with intermolecular van der Waal's forces. For instance, CNCs isolated from tunicate sea creatures have been successfully integrated into a rubbery ethylene oxide-epichlorohydrin copolymer matrix having a lower stiffness than conventional electrodes [127].

Another study reported the development of poly(vinyl acetate) (PVAc) and CNCs composites showing a dual responsive behavior. Upon exposure to physiological conditions, the composites are plasticized and the CNC network loses its stiffness capabilities due to the loss of hydrogen bonding. Once these composites were implanted in the pia mater of the cerebral cortex of a rat, the initial stiffness rapidly decreased matching that of the brain tissue [128, 129]. These adaptive microelectrodes implanted into a rat cortex for 8 weeks increased the cell density at the electrode–tissue interface. After 16 weeks of implantation, there was no neuron death surrounding PVAc/CNC implants as compared to PVAc-coated microelectrodes [130]. Another cortical implant in rats containing CNC/PVA and curcumin showed that after 4 weeks, curcumin promoted higher neuron survival and a more stable blood–brain barrier than the neat PVA controls [131].

8.5. Vascular grafts

BC-based implants have been developed to replace synthetic by-pass implants made of polytetrafluoroethylene, poly(ethylene terephthalate), polyethylene, and polyurethane.

Further, BC tubes have been successfully used to replace carotid arteries in rats, pigs, and sheep without any rejection after 4 weeks [127].

One study showed that the mechanical properties of CNC-PVA composites are similar to that of cardiovascular tissues, such as aorta and heart valve leaflets. For instance, the stress–strain properties for porcine aorta and heart valve tissue matches those of PVA-nanocellulose composites in the circumferential and the axial tissue directions [132].

The nanocellulose implants have been attached in the carotid artery of rats for 1 year, resulting in incorporation nanocellulose forming neointima and ingrowth of active fibroblasts. In another study, the grafts were used to successfully replace the carotid arteries of pigs [133]. Further, cellulose and chitosan composites have been successfully used to produce hollow tubes with a compliance compared to that of human coronary arteries showing potential for coronary artery bypass graft applications [134].

In one study, part of the carotid artery (4–6 mm) of a rat was replaced using BC and after 4 weeks, the BC complex was wrapped up with connective tissue and was infused with small vessels [28, 135]. BC porous surfaces have also been reported to maintain fiber network arrangement viable in endothelial cells for 20 days [136]. Further, the surface modification of BC by nitrogen-containing plasma improved cell adhesion and proliferation of the endothelial and neuroblast cells [137].

8.6. Medical implants

Medical implants must have mechanical characteristics as the tissue it replaces. It must also show nonthrombogenicity, sterilizability, durability, lesser degree of calcification, and good processability. The implant should be biocompatible with the host tissues in terms of chemical, mechanical, surface chemistry, and pharmacological properties.

BC is a good candidate for use as medical implants since it is nondegradable under physiological conditions and provides durable mechanical properties and chemical stability. One study showed that the mechanical properties of the BC gel with collagen meniscal implants were similar in magnitude to the ones of pig menisci [138].

Further, an ear-shaped BC prototype material showed suitable mechanical properties for ear cartilage replacement for a customized patient-specific ear shapes [139].

A nanocellulose membrane has also been implanted in the nasal dorsum of 22 rabbits as an excellent substitute of bone cartilage. After 6 months, residual inflammation was attributed to the surgical procedure itself and not to the cellulosic membrane [140].

The cartilage that covers the trochlear groove in dogs is composed of chondrocytes. Further, BC was utilized successfully in experimental trochleoplasty in dogs, showing advantage in respect to conventional treatment for osteochondral injuries [141]. Moreover, BC membrane was applied in the tissue formation of fibrocartilage ripe, resulting in a good integration of the newly formed tissue.

Other researchers have successfully incorporated BC and polytetrafluoroethylene (PTFE) membranes in rats to correct abdominal wall defects [142]. Further, BC implanted in the peritoneum of dogs formed an integrated net along the conjunctive tissue after 6 months [143].

On the other hand, the biggest challenge in dental applications is the loss of alveolar bone. For this reason, synthetic hydroxyapatite (HAP-91) was implanted in the dental cavities and covered by nanocellulose membranes. Nanocellulose promoted faster bone regeneration and resembled those of the original tissue after 50 days [144].

A bandage product derived from BC (Gengiflex®) restores the osseous defects. It consists of an inner layer of microbial cellulose, which offers rigidity to the membrane, and an outer layer of alkali cellulose. A greater amount of bone formation was present in bone defects protected by the BC membrane, when compared to the control sites [145, 146].

BC membranes were tested as physical barriers used to treat bone defects. In this scenario, two osseous defects (8 mm in diameter) were performed in each hind foot of four adult rabbits. After 3 months, the bone defects showed lamellar bone formation resulting in partial bone deposition [147].

8.7. Cell culture and scaffolds

The asymmetric structure of a scaffold is composed of a fine network of nanofibrils, which is similar to a collagen network, which promotes the adhesion and proliferation of muscle cells [97, 101]. BC has shown significantly higher levels of chondrocyte growth, suggesting the potential application of scaffolds for cartilage tissue engineering [148]. The beneficial properties of CNF are based on its unique nanofibrillar structure, mimicking properties of the extracellular matrix, and thus, a CNF scaffold promotes hepatocyte 3D cell culture without added bioactive components.

Nanocellulose and hydroxyapatite (HA) are both capable of bone replacement because of their properties, including biocompatibility with the human body, bioactivity, osteoconductivity, and noninflammatory properties [74]. Further, nanocellulose has also been soaked into HA to develop a composite scaffold for bone regeneration. Thus, CNC/HA scaffolds were prepared by absorption of HA onto the BC surface to induce nucleation of calcium-deficient HA. The presence of calcium-deficient HA crystals on the BC surface increased cell attachment and alkaline phosphatase activity on bone cells. Further, nanocellulose has been combined with polyacrylamide and gelatin, yielding hydrogels with improved toughness [149].

Moreover, enzymatically modified gelatin (EMG) and nanocellulose composites have been prepared to improve the rehydration properties and, thus, can be used as scaffold for the cornea tissue since the stromal cells are able to grow into the scaffold [150].

In one study, BC and poly(3-hydroxubutyrate-co-4-hydroxubutyrate) (P(3HB-co-4HB) composite scaffolds showed excellent biocompatibility in Chinese hamster lung (CHL) fibroblast cells [151]. Further, the BC and alginate composite (80:20 w/w) dried by supercritical carbon dioxide formed a nanoporous structure, which supports the proliferation of keratinocytes and gingival fibroblasts [152, 153].

In another study, nanocellulose/PEG composite scaffolds were prepared by soaking a nano-cellulose hydrogel with a PEG solution forming scaffold with improved thermal stability. Results indicated that the Young's modulus and tensile strength tended to decrease while the elongation at break had a slight increase. Thus, the prepared nanocellulose/PEG composite scaffolds were suitable for cell attachment [154].

The functionalization of the BC surface with recombinant proteins containing a bioactive peptide (IKVAV) and a carbohydrate-binding module (CBM3) has improved their biocom-patibility with neuronal and mesenchymal cells [155]. BC cross-linked with heparin is able to prevent the formation of blood clots [156]. A natural peptide called as polylysine (PLL) has been cross-linked to the surface of BC resembling the collagen fibers and composition of natural bone [157].

CNCs have been coated with 2-hydroxyethylmethacrylate and methacrylic functional groups forming hydrogels with excellent mechanical properties comparable to articular cartilage with hydrogel-like properties [158].

One study reported the creation composites based on BC and type I collagen (COL) for potential bone tissue engineering, in which collagen was covalently introduced into the BC network. Further, cell culture with osteogenic cells revealed that collagen did not affect cell adhesion and proliferation or its morphology [159]. Heparin and nanocellulose scaffolds have been prepared with anticoagulant properties for potential use in vascular tissue engineering [160].

Further, grafted zwitterionic carboxybetaine improved CNF membrane blood compatibility. In another study, dialdehyde BC membranes supported the epidermal cell adhesion and proliferation [161].

BC has also been used to treat wounds in diabetic foot ulcers. The mean time for 75% epithe-lization was achieved in 79 days, and BC shortened the epithelization time as compared to XeroformTM® Petrolatum gauze [162]. Another study showed a complete closure of the facial wound within 44 days with no significant signs of extensive scarring [121]. Further, the release of BC dressing from the wound is a painless operation due to the moisture still present in the cellulose structure [163].

A nanogel made of poly(*N*-isopropyl acrylamide-co-butyl methacrylate), BC, and a surfactant has been produced by emulsion polymerization. This nanogel showed a thermal responsive behavior from a swollen to shrunken gel with increasing temperature. This is explained by the decrease of hydrogen bonding interactions with temperature [164].

8.8. Antimicrobial activity

Nanocellulose intrinsically does not possess any antimicrobial property. Therefore, it needs to be functionalized with antimicrobial agents. For instance, chemical grafting of aminoalkyl groups [165], 2-benzyl-4- chlorophenol [166], and L-cysteine [167], onto the surface of the cellulose backbone has been reported [168]. In one study, a BC film was soaked in a benzal-

konium chloride solution, resulting in antimicrobial activity against *Staphylococcus aureus* and *Bacillus subtilis*, which are bacteria generally found on contaminated wounds [169].

The electrospun composite nanofiber membrane containing bis(*N*-chloro-2,2,6,6-tetramethyl-4-piperidinyl) sebacate (Cl-BTMP) showed significant antimicrobial activity against *S. aureus*, *Escherichia coli*, and *Pseudomonas aeruginosa* attributed to the aggregation of Cl-BTMP. Further, nanocomposites with curcumin rendered antimicrobial activity against *E. coli* and *S. aureus* over a period of 24 h [170].

The immersion of BC in a silver nitrate solution, followed by reduction of absorbed silver ions (Ag+) with sodium borohydride, formed metallic silver nanoparticles with antimicrobial activity against *E. coli* and *S. aureus* [169]. Further, aminoalkyl-grafted bacterial nanocellulose (BC-NH$_2$) membranes were prepared by hydrolysis of the silane derivative, adsorption of the hydrolyzed species onto BC nanofibrils, followed by a chemical condensation reaction. These BC–NH$_2$ membranes showed antimicrobial activity against *E. coli* and *S. aureus* after 24 h [167].

In another study, composites of CNF and chitin nanocrystals formed a 3D network with bactericidal activity against *E. coli*. On the other hand, the in situ sol-gel formation of silver and gold particles within CNF endowed it with antibacterial activity against *E. coli*, *S. aureus*, and *Klebsiella pneumonia* strains. The assembly of the CNFs and silver nanoparticle (AgNP) composites occurs through electrostatic interactions. Another strategy of incorporation of silver is through magnetic interaction where the 3D structure of cellulose provides plenty of sites for heterogeneous nucleation of magnetite rendering a high antimicrobial activity against *E. coli* and *B. subtilis* [2]. Further, nanocomposite films prepared by the addition of cellulose nanocrystals, with silver nanoparticles, in a PLA matrix generate an antibacterial film against *S. aureus* and *E. coli* [171]. Silver ions interfere with the respiratory chain causing a decrease in bacterial viability [172–174]. Moreover, Ag and Au nanoparticles have been synthesized on CNC using cationic surfactants such a CTABr [175, 176].

In one study, BC was first homogenized with a ferric and ferrous salt mixture followed by soaking in dopamine and silver nitrate solution. The resulting magnetic silver/BC nanocomposites had antimicrobial activity against *E. coli* and *B. subtilis* were developed.

8.9. Drug delivery

The abundant surface hydroxyl groups in nanocellulose provide a site for the surface modification by a variety of methods. Surface modification modulates the loading and release of nonionized or hydrophobic drugs that would not normally bind to nanocellulose. For instance, poly(caprolactone) chains might be conjugated onto CNC for drug release [31].

PVA and methyl cellulose form aninterprenetrating polymer network through cross-linking with epichlorohydrin and serve as a carrier to load a drug for controlled release [31]. Further, coating of CNC with a cationic surfactant such as cetyltrimethylammonium bromide (CTABr) has been useful to load significant quantities of anticancer agents for controlled released [177–179]. In one study, nanoparticles of itraconazole were stabilized by the nanostructured cellulose matrix during freeze-drying and storage increasing its dissolution rate and in vivo performance [177].

On the other hand, spray-dried CNFs were produced in order to increase the long-term stability of drugs due to a better ability to pack having a low porosity and forming fast disintegrating tablets [179]. Further, BC membranes loaded with lidocaine rendered lower permeation rates in the skin than traditional drug delivery systems. The greatest advantage of the BC membrane is the combination of its wound healing capacity and the ability to absorb exudates with the release of antimicrobial and anti-inflammatory drugs [180].

In another study, freeze-dried BC and serum albumin composites were investigated as potential drug delivery systems for proteins [110]. In one report, CNC was oxidized with periodic acid to graft a spacer molecule (aminobutyric acid), and then syringyl alcohol was attached. In another investigation, calcium peroxide (CPO) was embedded into highly porous CNCs to produce H_2O_2, whereas catalase was added to convert the generated H_2O_2 to O_2, increasing cell survival up to 5 days [181].

Weng et al. created biodegradables cellulose microspheres loaded with doxorubicin for arterial embolization applications. They showed a burst release profile within 8 h followed by a release plateau over a 24-h period in rabbits [182].

Further, docetaxel-loaded CMC-based nanoparticles have been produced for enhanced cytotoxicity against cancer cells releasing 100% of drug within 3 weeks inhibiting 90% of tumor growth [183]. In another study, CMC gels were produced by polymerization of oligo(ethylene oxide)-methacrylate (OEOMA) in the presence of CNC. These gels have a dual drug release in response to acidic pH and thiol-reducing agents [184].

Zoppe and collaborators applied CNC-based systems as viral inhibitors (alphavirus infectivity) and suggested that CNC can be used for inhibition of HIV [185].

9. Conclusion

The attractive properties of nanocellulosic materials such as biodegradability, biocompactibility, renewability, low density, high strength, good stiffness, low thermal expansion, and high aspect ratio make them suitable for biomedical applications. For this reason, the number of publications and patents related to these applications has skyrocketed in the last 5 years. However, a great effort has still to be made to reduce the high cost involved with the production process of nanocellulose intended for biomedical used.

Author details

John Rojas*, Mauricio Bedoya and Yhors Ciro

*Address all correspondence to: jrojasca@gmail.com

Department of Pharmacy, School of Pharmaceutical Chemistry, University of Antioquia, Medellín, Columbia

References

[1] Li J, Xu QH, Jin LQ. Research development on hydrophobic modification of cellulose nanofibrils. Adv Mater Res [Internet]. 2013;785–786:440–3. Available from: http://www.scientific.net/AMR.785-786.440

[2] Robles NB. Tailoring cellulose nanofibrils for advanced materials. KTH Royal Institute of Technology; 2014. p. 82.

[3] Zheng H. Production of fibrillated cellulose materials—effects of pretreatments and refining strategy on pulp properties. Aalto University; 2014. p. 74.

[4] Deepa B, Abraham E, Cordeiro N, Mozetic M, Mathew Ap OK, Faria M, Thomas S, Pothan LA. Utilization of various lignocellulosic biomass for the production of nanocellulose: a comparative study. Cellulose. 2015;22(2):1075–90.

[5] Lin SP, Loira Calvar I, Catchmark JM, Liu JR, Demirci A, Cheng KC. Biosynthesis, production and applications of bacterial cellulose. Cellulose. 2013;20(5):2191–219.

[6] Lee KY, Buldum G, Mantalaris A, Bismarck A. More than meets the eye in bacterial cellulose: biosynthesis, bioprocessing, and applications in advanced fiber composites. Macromol Biosci. 2014;14(1):10–32.

[7] Lee KY, Tamelin T, Schulter K, Kiliskinen H, Samela J, Bismarck A. High performance cellulose nanocomposites: comparing the reinforcing ability of bacterial cellulose and nanofibrillated cellulose. ACS Appl Mater Interfaces. 2012;4(8):4078–86.

[8] Rajwade JM, Paknikar KM, Kumbhar J V. Applications of bacterial cellulose and its composites in biomedicine. Appl Microbiol Biotechnol [Internet]. 2015;ASAP. Available from: http://link.springer.com/10.1007/s00253-015-6426-3

[9] De Campos A, Correa AC, Cannella D, Teixeria EM, Marconcini JM, Dufresne A, Mattoso LHC, Cassland P, Sanadi AR. Obtaining nanofibers from curauá and sugarcane bagasse fibers using enzymatic hydrolysis followed by sonication. Cellulose. 2013;20(3):1491–500.

[10] Liu LL, Tian YB, Tang CC, Zhang H, Liu X. The preparation of nanocrystalline cellulose by acid and enzymatic method. Food Ferment Ind. 2011;

[11] De campos A, Correa AC, Cannella D, Teixeira EM, Marconcini JM, Dufrense A, Mattoso LHC, Cassland P, Sanadi AR. Obtaining nanofibers from curauá and sugarcane bagasse fibers using enzymatic hydrolysis followed by sonication. Cellulose. 2013;20(3):1491–500.

[12] Anderson SR, Esposito D, Gillete W, Zhu JY, Baxa U, McNeil SE. Enzymatic preparation of nanocrystalline and microcrystalline cellulose. Tappi J. 2014;13(5):35–42.

[13] Lai C, Zhang S, Sheng L, Liao S, Xi T, Zhang Z. TEMPO-mediated oxidation of bacterial cellulose in a bromide-free system. Colloid Polym Sci. 2013;291(12):2985–92.

[14] Lin D, Li R, Lopez-Sanchez P, Li Z. Physical properties of bacterial cellulose aqueous suspensions treated by high pressure homogenizer. Food Hydrocoll. 2015;44:435–42.

[15] Siqueira G, Tapin-Lingua S, Bras J, da Silva Perez D, Dufresne A. Morphological investigation of nanoparticles obtained from combined mechanical shearing, and enzymatic and acid hydrolysis of sisal fibers. Cellulose. 2010;17(6):1147–58.

[16] Amiralian N, Annamalai PK, Memmott P, Taran E, Schmidt S, Martin DJ. Easily deconstructed, high aspect ratio cellulose nanofibres from *Triodia pungens*; an abundant grass of Australia's arid zone. RSC Adv. 2015;5:32124–32.

[17] Lu H, Gui Y, Zheng L, Liu X. Morphological, crystalline, thermal and physicochemical properties of cellulose nanocrystalsobtained from sweet potato residue. Food Res Int. 2013;50(1):121–8.

[18] Dos Santos RM, Flauzino WP, Silvério HA, Ferreira D, Oliveira N, Pasquin D. Cellulose nanocrystals from pineapple leaf, a new approach for the reuse of this agrowaste. Ind Crops Prod. 2013;50:707–14.

[19] Deepa EA, Koshy RR, Pothan LA, Thomas S. Extraction and characterization of cellulose nanofibers from banana plant. Handbook of Polymer Nanocomposites Processing, Performance and Application. 2015. p. 65–80.

[20] Flauzino WP, Alves H, Oliveira N, pasquini D. Extraction and characterization of cellulose nanocrystals from agro-industrial residue–soy hulls. Ind Crops Prod. 2013;42:480–8.

[21] Hua K, Carlsson DO, Ålander E, Lindström T, Strømme M, Mihranyan A, Ferraz N S. Translational study between structure and biological response of nanocellulose from wood and green algae. RSC Adv. 2014;4:2892–903.

[22] Rahimi M, Behrooz R. Effect of cellulose characteristic and hydrolyze conditions on morphology and size ofnanocrystal cellulose extracted from wheat straw. Int J Polym Mater. 2011;60(8):529–41.

[23] Li R, Fei J, Cai Y, Li Y, Feng J, Yao J. Cellulose whiskers extracted from mulberry: a novel biomass production. Carbohydr Polym. 2009;76(1):94–9.

[24] Hsieh YL. Cellulose nanocrystals and self-assembled nanostructures from cotton, rice straw and grape skin: a source perspective. J Mater Sci. 2013;48(22):7837–46.

[25] Xu C, Zhu S, Xing C, Li D, Zhu N, Zhou H. Isolation and properties of cellulose nanofibrils from coconut palm petioles by different mechanical process. PLoS One. 2015;10(4).

[26] Mao J, Osorio-Madrazo A, Laborie MP. Preparation of cellulose I nanowhiskers with a mildly acidic aqueous ionic liquid: reaction efficiency and whiskers attributes. Cellulose. 2013;20(4):1829–40.

[27] Fortunati E, Puglia D, Monti M, Peponi L, Santulli C, Kenny JM, Torre L. Extraction of cellulose nanocrystals from *Phormium tenax* fibres. J Polym Env. 2013;21(2):319–28.

[28] Lin N, Dufrense A. Nanocellulose in biomedicine: current status and future prospect. Eur Polym J. 2014;59:302–25.

[29] Jonoobi M, Mathew AP, Oksman K. Producing low-cost cellulose nanofiber from sludge as new source of raw materials. Ind Crops Prod. 2012;40(1):232–8.

[30] Li Q. Nanocellulose: preparation, characterization, supramolecular modeling, and its life cycle assessment. Virginia Polytechnic Institute & State University; 2012. p. 186.

[31] kalia S, Boufi S, Celli A, Kango S. Nanofibrillated cellulose: surface modification and potential applications. Colloid Polym Sci. 2014;292(1):5–31.

[32] Isogai A. Wood nanocelluloses: fundamentals and applications as new bio-based nanomaterials. J Wood Sci. 2013;59(6):449–59.

[33] Wang Q, Zhao X, Zhu JY. Kinetics of strong acid hydrolysis of a bleached kraft pulp for producing cellulose nanocrystals (CNCs). Ind Eng Chem Res. 2014;53(27):11007–14.

[34] Li J, Wei X, Wang Q, Chen J, Chang G, Kong L, Su J, Liu Y. Homogeneous isolation of nanocellulose from sugarcane bagasse by high pressure homogenization. Carbohydr Polym. 2012;90(4):1609–13.

[35] Chaker A, Mutjé P, Vilar MR, Boufi S. Agriculture crop residues as a source for the production of nanofibrillated cellulose with low energy demand. Cellulose. 2014;21(6):4247–59.

[36] Liu LL, Tian YB, Tang CC, Zhong C, Liu X. Preparation of nanocrystalline cellulose from soybean dregs by acid hydrolysis followed by high-pressure homogenization. Food Sci. 2011;

[37] Wang Y, Wei X, Li J, Wang Q, Wang F, Kong L. Homogeneous isolation of nanocellulose from cotton cellulose by high pressure homogenization. J Mater Chem Eng. 2013;1:49–52.

[38] Hassan ML, Mathew AP, Hassan EA, El-Wakil NA OK. Nanofibers from bagasse and rice straw: process optimization and properties. Wood Sci Technol. 2012;46(1):193–205.

[39] Xie C, Liu ZM, Wu P, Fang GZ, Zhao X. Optimization of preparation technology of alkali pretreated reed pulp nano-cellulose. Chem Ind For Prod. 2013;

[40] Stelte W, Sanadi AR. Preparation and characterization of cellulose nanofibers from two commercial hardwood and softwood pulps. Ind Eng Chem Res [Internet]. 2009;48(24):11211–9. Available from: http://dx.doi.org/10.1021/ie9011672

[41] He W, Jiang X, Sun F, Xu X. Extraction and characterization of cellulose nanofibers from *Phyllostachys nidularia munro* via a combination of acid treatment and ultrasonication. BioResources. 2014;9(4):6876–87.

[42] Chen W, Yu H, Liu Y, Hai Y, Zhang M, Chen P. Isolation and characterization of cellulose nanofibers from four plant cellulose fibers using a chemical-ultrasonic process. Cellulose. 2011;18(2):433–42.

[43] Frey MW. Electrospinning cellulose and cellulose derivatives. Polym Rev. 2008;48(2): 378–91.

[44] Satyamurthy P, Jain P, Balasubramanya RH, Vigneshwaran N. Preparation and characterization of cellulose nanowhiskers from cotton fibres by controlled microbial hydrolysis. Carbohydr Polym. 2011;83(1):122–9.

[45] Sacui LU, Nieuwendaal RC, Burnett DJ, Stranick SJ, Jorfi M, Weder C, Foster EJ, Olsson RT, Gilman JW. Comparison of the properties of cellulose nanocrystals and cellulose nanofibrils isolated from bacteria, tunicate, and wood processed using acid, enzymatic, mechanical, and oxidative methods. ACS Appl Mater Interfaces. 2014;6(9):6127–38.

[46] Sinko R, Qin X, Keten S. Interfacial mechanics of cellulose nanocrystals. MRS Bull [Internet]. 2015;40(04):340–8. Available from: http://www.journals.cambridge.org/abstract_S0883769415000676

[47] Habibi Y, Lucia LA, Rojas OJ. Cellulose nanocrystals: chemistry, self-assembly, and applications. Chem Rev. 2010;110(6):3479–500.

[48] yue Y, Zhou C, French AD, Xia G, Han G, Wang Q, Wu Q. Comparative properties of cellulose nano-crystals from native and mercerized cotton fibers. Cellulose. 2012;29(4):1173–87.

[49] Charreau H, L. Foresti M, Vazquez A. Nanocellulose patents trends: a comprehensive review on patents on cellulose nanocrystals, microfibrillated and bacterial cellulose. Recent Pat Nanotechnol. 7(1):56–80.

[50] Ioelovich M. Optimal conditions for isolation of nanocrystalline cellulose particles. Nanosci Nanotechnol. 2012;2(2):9–13.

[51] Sadeghifar H, Filpponen I, Clarke SP, Brougham DF, Argypoulos DS. Production of cellulose nanocrystals using hydrobromic acid and click reactions on their surface. J Mater Sci. 2011;46(22):7344–55.

[52] Brito BSL, Pereira FV, Putaux JL, Jean B. Preparation, morphology and structure of cellulose nanocrystals from bamboo fibers. Cellulose. 2012;19(5):1527–36.

[53] Zhang J, Elder TJ, Pu Y, Ragauskas AJ. Facile synthesis of spherical cellulose nanoparticles. Carbohydr Polym. 2007;3(25):607–11.

[54] Cheng ZL, Xu QH, Gao Y. Research progress in nano-cellulose modification. Adv Mater Res. 2012;627:859–63.

[55] Hai LV, Son HN, Seo YB. Physical and bio-composite properties of nanocrystalline cellulose from wood, cotton linters, cattail, and red algae. Cellulose. 2015;22(3):1789–98.

[56] Yang D, Peng XW, Zhong LX, Cao XF, Chen W, Sun RC. Effects of pretreatments on crystalline properties and morphology of cellulose nanocrystals. Cellulose. 2013;20(5):2427–37.

[57] Yingkamhaeng N, Sukyai P. The potential of mango peel utilization for cellulose extraction by hydrothermal pretreatment. Annual Meeting of the Thai Society for Biotechnology and International Conference. 2014.

[58] Penttilä PA, Várnai A, Fernández M, Kontro I, Liljeström V, Lindner P, Siika-aho M, Viikari L, Serimaa R. Small-angle scattering study of structural changes in the microfibril network of nanocellulose during enzymatic hydrolysis. Cellulose. 2013;20(3): 1031–40.

[59] Kargarzadeh H, Ahmad I, Abdullah I, Dufrense A, Zainudin SY, Sheltami RM. Effects of hydrolysis conditions on the morphology, crystallinity, and thermal stability of cellulose nanocrystals extracted from kenaf bast fibers. Cellulose. 2012;19(3):855–66.

[60] Lam E, Male KB, CHong JH, Leung ACW, Luong JHT. Applications of functionalized and nanoparticle-modified nanocrystalline cellulose. Trends Biotechnol. 2012;30(5): 283–90.

[61] Jiang F, Hsieh YL. Super water absorbing and shape memory nanocellulose aerogels from TEMPO-oxidized cellulose nanofibrils via cyclic freezing–thawing. J Mater Chem. 2014;2:350–9.

[62] Cao X, Ding B, Yu J, Al-Deyab SS. Cellulose nanowhiskers extracted from TEMPO-oxidized jute fibers. Carbohydr Polym. 2012;90(2):1075–80.

[63] Fujisawa S, Okita S, Fukuzumi H, Saito T, Isogai A. Preparation and characterization of TEMPO-oxidized cellulose nanofibril films with free carboxyl groups. Carbohydr Polym. 2011;84(1):579–83.

[64] Kekäläinen K, Liimatainen H, Biale F, Holzforschung JN. Nanofibrillation of TEMPO-oxidized bleached hardwood kraft cellulose at high solids content. Holzforschung. 2015;1–12.

[65] Pettersen SR. Cross-linking oxidized cellulose nanofibrils for the formation of stable hydrogel structures. Institutt for kjemisk prosessteknologi; 2013.

[66] Mishra SP, Thirree J, Manent AS, Chabot B, Daneault C. Ultrasound-catalyzed TEM-PO-mediated oxidation of native cellulose for the production of nanocellulose: effect of process variables. BioResources. 2011;6(1):121–43.

[67] Li Q, Renneckar S. Molecularly thin nanoparticles from cellulose: isolation of sub-microfibrillar structures. Cellulose. 2009;16(6):1025–32.

[68] Castro-Guerrero CF, Gray DG. Chiral nematic phase formation by aqueous suspensions of cellulose nanocrystals prepared by oxidation with ammonium persulfate. Cellulose. 2014;21(4):2567–77.

[69] Xiao YT, Chin WL, Abd Hamind SB. Facile preparation of highly crystalline nanocellulose by using ionic liquid. Adv Mater Res. 2015;1087:106–10.

[70] Lazko J, Sénéchal T, Landercy N, Dangreau L, Raquez JM, Dubois P. Well defined thermostable cellulose nanocrystals via two-step ionic liquid swelling-hydrolysis extraction. Cellulose. 2014;21(6):4195–207.

[71] Hassan ML. Bagasse and rice straw nanocellulosic materials and their applications. Handbook of Polymer Nanocomposites Processing, Performance and Application. 2015. p. 47–64.

[72] Laurén P. Small-animal SPECT/CT and nanofibrillar cellulose hydrogels: a preclinical evaluation of a potential novel biomaterial application. University of Helsinki; 2013. p. 71.

[73] Wicaksono R, Syamsu K, Yuliasih I, Nasir M. Cellulose nanofibers from cassava bagasse: characterization and application on tapioca-film. Chem Mater Res. 2013;3(13): 79–87.

[74] Gatenholm P. Bone Healing Grafts Fabricated by Nanoscale Assembly of Biological Building Blocks. 2010 p. 126–32.

[75] Missoum K. Modification chimique de surface de NanoFibrilles de Cellulose (NFC) [Internet]. 2012. Available from: http://www.theses.fr/2012GRENI105/document

[76] Morais JPS, Rosa MF, Souza MSM, Alexandrino LC, Ribeiro AC. Processo de obtenção de nanocristais de celulose a partir do línter de algodão. Pesquisa e Desenvolvimento. 2012 p. 22.

[77] De Morais E, Corrêa AC, Manzoli A, Leite FL, de Oliveira CR, Mattoso LHC. Cellulose nanofibers from white and naturally colored cotton fibers. Cellulose. 2010;17(3): 595–606.

[78] Gamelas JAF, Pedrosa J, Lourenco AF, Ferreria PJ. Surface properties of distinct nanofibrillated celluloses assessed by inverse gas chromatography. Colloids Surf A Physicochem Eng Asp. 2015;469:36–41.

[79] Mariño M, Da silva LP, Durán N, Tasic L. Enhanced materials from nature: nanocellulose from citrus waste. Molecules. 2015;20:5908–23.

[80]   Baheti VK, Abassi R, Militky J. Ball milling of jute fibre wastes to prepare nanocellulose. World J Eng. 2012;9(1):45–50.

[81]   Baheti V, Abbasi R, Militky J A. Optimisation of ball milling parameters for refinement of waste jute fibres to nano/micro scale in dry conditions. J Text Eng. 2013;59(5): 87–92.

[82]   Kumar A, Negi YS, Choudhary V, Bhardwaj NK. Characterization of cellulose nanocrystals produced by acid-hydrolysis from sugarcane bagasse as agro-waste. J Mater Physic Chem. 2014;2(1):1–8.

[83]   Do Nascimiento DM, Norões AKM, Souza NF, Alexandre LC, Morais JPS, Mazzeto SE, Rosa MF. Thermal and structural characteristics of waste derived biomass for potential application in nanomaterials. 7th International Symposium on Natural Polymers and Composites.

[84]   Chen Y, Wu Q, Huang B, Huang M, Ai X. Isolation and characteristics of cellulose and nanocellulose from lotus leaf stalk agro-wastes. BioResources. 2015;10(1):684–96.

[85]   Kalita E, Nath BK, Agan F, More V, Deb P. Isolation and characterization of crystalline, autofluorescent, cellulose nanocrystals from saw dust wastes. Ind Crops Prod. 2014;

[86]   Li Y, Zhu H, Xu M, Zhuang Z, Xu M, Dai H. High yield preparation method of thermally stable cellulose nanofibers. BioResources. 2014;9(2):1986–97.

[87]   Peng Y, Gardner DJ, Han Y, Cai Z, Tshabala MA. Drying cellulose nanofibrils: in search of a suitable method. Cellulose. 2012;19(1):91–102.

[88]   Fairman E. Avoiding Aggregation During Drying and Rehydration of Nanocellulose. University of Maine; 2014. p. 60.

[89]   Peng Y, Gardner DJ, Han Y, Kiziltas A, Cai Z, Tshabalala MA. Influence of drying method on the material properties of nanocellulose I: thermostability and crystallinity. Cellulose. 2013;20(5):2379–92.

[90]   Belbekhouche S, Bras J, Siqueira G, Chappey C, Lebrun L, Khelifi B, Marais S, Dufresne A. Water sorption behavior and gas barrier properties of cellulose whiskers and microfibrils films. Carbohydr Polym. 2011;83(4):1740–8.

[91]   Majoinen J, Kontturi E, Ilkkala O, Gray DG. SEM imaging of chiral nematic films cast from cellulose nanocrystal suspensions. Cellulose. 2012;19(5):1599–605.

[92]   Dankovich TA, Gray DG. Contact angle measurements on smooth nanocrystalline cellulose (I) thin films. J Adhes Sci Technol. 2011;25(6–7):699–708.

[93]   Wang Y, Heim LO, Xu Y, Buntkowsky G, Zhang K. Transparent, stimuli responsive films from cellulose based organogel nanoparticles. Adv Funct Mater. 2015;25:1434–41.

[94] Chen W, Li Q, Wang Y, Yi X, Zeng J, Yu H, Liu Y, Li J. Comparative study of aerogels obtained from differently prepared nanocellulose fibers. Chem Sus Chem. 2014;7:154–61.

[95] Zhang ZL, Wang WJ, Shao ZQ, LV SY. Rheological properties of cellulose nanocrystals suspension at different pH. Nanosci Nanotechnol. 2012;

[96] Li MC, Wu Q, Song K, Lee S, Qing Y, Wu Y. Cellulose nanoparticles: structure–morphology–rheology relationship. ACS Sustain Chem Eng. 2015;3(5):821–32.

[97] Dugan JM, Gough JE, Eichhorn SJ. Bacterial cellulose scaffolds and cellulose nanowhiskers for tissue engineering. Nanomedicine. 2013;8(2):287–98.

[98] Jeong SL, Lee SE, Yang H, Jin YH, Park CS, Park YS. Toxicologic evaluation of bacterial synthesized cellulose in endothelial cells and animals. Mol Cell Toxicol. 2010;6(4): 373–80.

[99] Wang ZL, Jia YY, Shi Y, Cong DL, Chen YY, Jia SR, Zhou YL. Research on characterization and biocompatibility of nano-bacterial cellulose membrane. Chem J Chinese Univ. 2009;30(8):1553–8.

[100] Edwards JV, Prevost N, French A, Concha M, De Lucca A, Wu Q. Nanocellulose-based biosensors: design, preparation, and activity of peptide-linked cotton cellulose nanocrystals having fluorimetric and colorimetric elastase detection sensitivity. Engineering. 2013;5(9A):20–8.

[101] He X, Xiao Q, Lu C, Wang Y, Zhang X, Zhao J, Zhang W, Zhang W, Deng Y. Uniaxially aligned electrospun all-cellulose nanocomposite nanofibers reinforced with cellulose nanocrystals: scaffold for tissue engineering. Biomacromolecules. 2014;15(2): 618–27.

[102] Tasset S, Cathala B, Bizot H, Capron I. Versatile cellular foams derived from CNC-stabilized Pickering emulsions. RSC Adv. 2014;4:893–8.

[103] Dai D, Fan M, Collins P. Fabrication of nanocelluloses from hemp fibers and their application for the reinforcement of hemp fibers. Ind Crops Prod. 2013;44:192–9.

[104] Kumar S, Hofmann M, Steinmann B, Foster EJ, Weder C. Reinforcement of stereolithographic resins for rapid prototyping with cellulose nanocrystals. ACS Appl Mater Interfaces. 2012;4(10):5399–407.

[105] Ibrahim MM, El-Zawawy WK. Extraction of cellulose nanofibers from cotton linter and their composites. Handbook of Polymer Nanocomposites Processing, Performance and Application. 2015. p. 145–64.

[106] Syverud K, Pettersen SR, Draget K, Chinga-Carrasco G. Controlling the elastic modulus of cellulose nanofibril hydrogels—scaffolds with potential in tissue engineering. Cellulose. 2015;22(1):473–81.

[107] Empson YM, Ekwueme EC, Hong JK, Paynter DM, Kwansa AL. High elastic modulus nanoparticles: a novel tool for subfailure connective tissue matrix damage. Transl Res. 2014;164(3):244–57.

[108] Mahmoud KA, Mena JA, Male KB, Hrapovic S, Kamen A, Luong JHT. Effect of surface charge on the cellular uptake and cytotoxicity of fluorescent labeled cellulose nanocrystals. ACS Appl Mater Interfaces [Internet]. 2010;2(10):2924–32. Available from: http://dx.doi.org/10.1021/am1006222

[109] Zhang Y, Nypelö T, Salas C, Arboleda J, Hoeger IC, Rojas OJ. Cellulose nanofibrils: from strong materials to bioactive surfaces. J Renew Mater. 2013;1(3):195–211.

[110] Orelma H, Filpponen I, Johansson LS, Österberg M, Rojas OJ. Surface functionalized nanofibrillar cellulose (NFC) film as a platform for immunoassays and diagnostics. Biointerphases. 2012;7(61):1–12.

[111] Andrade FK, Moreira SMG, Domingues L, Gama FMP. Improving the affinity of fibroblasts for bacterial cellulose using carbohydrate-binding modules fused to RGD. J Biomed Mater Res Part A. 2010;92A(1):9–17.

[112] Fu L, Zhang J, Yang G. Present status and applications of bacterial cellulose-based materials for skin tissue repair. Carbohydr Polym. 2013;92(2):1432–42.

[113] Yang H, Gurgel P, Carbonell RG. Hexamer peptide affi nity resins that bind the Fc region of human immunoglobulin G. J Pept Rees. 2006;66:120–37.

[114] Edwards JV, Prevost N, Sethumadhavan K, Ullah A, Condon B. Peptide conjugated cellulose nanocrystals with sensitive human neutrophil elastase sensor activity. Cellulose. 2013;20(3):1223–35.

[115] Liu H, Wang D, Song Z, Shang S. Preparation of silver nanoparticles on cellulose nanocrystals and the application in electrochemical detection of DNA hybridization. Cellulose. 2011;18(1):67–74.

[116] Mangalam AP, Simonsen J, Benight, Albert S. Cellulose/DNA hybrid nanomaterials. Biomacromolecules [Internet]. 2009;10(3):497–504. Available from: http://dx.doi.org/10.1021/bm800925x

[117] Dong S, Cho HJ, Lee YW, Roman M. Synthesis and cellular uptake of folic acid-conjugated cellulose nanocrystals for cancer targeting. Biomacromolecules [Internet]. 2014;15(5):1560–7. Available from: http://dx.doi.org/10.1021/bm401593n

[118] Pereira MM, Rapsoso NRB, Brayner R, Teixeira EM, Oliveira V, Quintão CCR, Camargo LSA, Mattoso LHC, Brandão HM. Cytotoxicity and expression of genes involved in the cellular stress response and apoptosis in mammalian fibroblast exposed to cotton cellulose nanofibers. Nanotechnology. 2013;24(7):75–103.

[119] Czaja W, Krystynowicz A, Bielecki S, Jr. RMB. Microbial cellulose—the natural pow-er to heal wounds. Biomaterials [Internet]. 2006;27(2):145–51. Available from: http://www.sciencedirect.com/science/article/pii/S0142961205007040

[120] MacNeil. Progress and opportunities for tissue-engineered skin. Nature [Internet]. 2007;445(7130):874–80. Available from: http://www.scopus.com/inward/record.url?eid=2-s2.0-33847256045&partnerID=40&md5=1fdd157f69a1cc6a2901c5930d385526

[121] Czaja WK, Young DJ, Kawecki M, Brown RM Jr. The future prospects of microbial cellulose in biomedical applications. Biomacromolecules. 2007;8(1):1–12.

[122] Fu L, Zhang Y, Li C, Zhihong W, Zhuo Q, Huang X, Qiu G, Zhou P, Yang G. Skin tissue repair materials from bacterial cellulose by a multilayer fermentation method. J Mater Chem. 2012;22:12349–57.

[123] Nwe N, Furuike T, Tamura H. Selection of a biopolymer based on attachment, mor-phology and proliferation of fibroblast NIH/3T3 cells for the development of a biode-gradable tissue regeneration template: alginate, bacterial cellulose and gelatin. Process Biochem. 2010;45(4):457–66.

[124] Ul-Islam M, Khan T, Park JK. Water holding and release properties of bacterial cellu-lose obtained by in situ and ex situ modification. Carbohydr Polym. 2012;88(2):596–603.

[125] Kalia S, Dufresne A, Cherian BM, Kaith BS, Avérous L, Njuguna J, Nassiopoulos E. Cellulose-based bio- and nanocomposites: a review. Int J Polym Sci. 2011;2011:1–35.

[126] Helenius G, Backdahl H, Bodin A, Nannmark U, Gatenholm P, Risberg B. In vivo bi-ocompatibility of bacterial cellulose. J Biomed Mater Res A. 2006;76(2):431–8.

[127] Jorfi M, Foser J. Recent advances in nanocellulose for biomedical applications. J Appl Polym Sci. 2015;132(14):1–19.

[128] Shanmuganathan K, Capadona JR, Rowan SJ, Weder C. Stimuli-responsive mechani-cally adaptive polymer nanocomposites. ACS Appl Mater Interfaces. 2010;2(1):165–74.

[129] Shanmuganathan K, Capadona JR, Rowan SJ, Weder C. Biomimetic mechanically adaptive nanocomposites. 2010. 35AD;1–2(212–222).

[130] Nguyen JK, Park DJ, Skousen JL, Hess-Dunning AE, Tyler DJ, Rowan SJ, Weder C, Capadona JR. Mechanically-compliant intracortical implants reduce the neuroinflam-matory response. J Neural Eng. 2014;11(5):1–15.

[131] Potter KA, Jorfi M, Householder KT, Foster EJ, Weder C, Capadona JR. Curcumin-releasing mechanically adaptive intracortical implants improve the proximal neuro-nal density and blood–brain barrier stability. Acta Biomater. 2014;10(5):2209–22.

[132] Millon LE, Wan WK. The polyvinyl alcohol-bacterial cellulose system as a new nano-composite for biomedical application. J Biomed Mater Res. 2006;79(2):245–53.

[133] Schumann DA, Wippermann J, Klemm DO. Artificial vascular implants from bacterial cellulose: preliminary results of small arterial substitutes. Cellulose. 2009;16(5): 877–85.

[134] Azevedo EP, Retarekar R, Raghavan ML, Kumar V. Mechanical properties of cellulose: chitosan blends for potential use as a coronary artery bypass graft. J Biomater Sci Polym Ed. 2013;24(3):239–52.

[135] Klemm D, Schumann D, Udhardt U, Marsch S. Bacterial synthesized cellulose—artificial blood vessels for microsurgery. Prog Polym Sci. 2001;26:1561–603.

[136] Berti F V, Rambo CR, Dias PF, Porto LM. Nanofiber density determines endothelial cell behavior on hydrogel matrix. Mater Sci Eng C. 2013;33:4684–91.

[137] Pertile RAN, Andrade FK, Jr. CA, Gama M. Surface modification of bacterial cellulose by nitrogen-containing plasma for improved interaction with cells. Carbohydr Polym [Internet]. 2010;82(3):692–8. Available from: http://www.sciencedirect.com/ science/article/pii/S0144861710004352

[138] Bodin A, Concaro S, Brittberg M, Gatenholm P. Bacterial cellulose as a potential meniscus implant. J Tissue Eng Regen Med. 2007;1(5):406–8.

[139] Nimeskern L, Martínez Ávila H, Sundberg J, Gatenholm P, Müller R, Stok KS. Mechanical evaluation of bacterial nanocellulose as an implant material for ear cartilage replacement. J Mech Behav Biomed Mater. 2013;22:12–21.

[140] Amorim WL, Costa HO, Souza FC, Castro MG, Silva L. Experimental study of the tissue reaction caused by the presence of cellulose produced. Braz J Otorhinolaryngol. 2009;75(2):200–7.

[141] Iamaguti LS, Branda˜o CVS, Minto BW. Handbook of Polymer Nanocomposites. Processing, Performance and Application [Internet]. 2015. Available from: http:// link.springer.com/10.1007/978-3-642-38649-7

[142] FalcÃ\poundso SC, EvÃ\textordfemeninencio Neto J, Coelho AR de B. Incorporation by host tissue of two biomaterials used as repair of defects produced in abdominal wall of rats. Acta Cir Bras [Internet]. scielo; 2008;23:78–83. Available from: http:// www.scielo.br/scielo.php?script=sci_arttext&pid=S0102-86502008000100013&nrm=iso

[143] Nemetz AP, Loures DRR, Coelho JCU. Efeito estrutural da utilização de celulose biossintética e politetrafluoretileno expandido como substitutos do peritônio em cães. Arq Bras Cir Dig. 2001;14(2):139–42.

[144] Silva EC. Hidroxiapatita Sintética em alvéolo dentário após exodontia em Felis catus: estudo clínico, radiológico e histomorfométrico. Universidad Federal de Vicosa; 2009.

[145] Novaes AB Jr, Novaes AB. IMZ implants placed into extraction sockets in association with membrane therapy (Gengiflex) and porous hydroxyapatite: a case report. Int J Oral Maxillofac Implant. 1992;7(4):563–540.

[146] Salata LA, Craig GT, Brook IM. In vivo evaluation of a new memnbrane (Gengiflex) for guided bone regeneratien (GBR),". J Dent Res. 1995;74(3):825.

[147] Macedo NL, Matuda FS, Macedo LGS, Monteiro ASF, Valera MC, Carvalho YR. Evaluation of two membranes in guided bone tissue regeneration: histological study in rabbits. Brazilian J Oral Sci. 2004;3(8):395–400.

[148] Svensson A, Nicklasson E, Harrah T, Panilaitis B, Kaplan DL, Brittberg M, Gatenholm P. Bacterial cellulose as a potential scaffold for tissue engineering of cartilage. Biomaterials. 2005;26:419–31.

[149] Wan YZ, Hong L, Jia RS, Huang Y, Zhu Y, Wang YL, Jiang HJ. Synthesis and characterization of hydroxyapatite-bacterial cellulose nanocomposites. Compos Sci Technol. 2006;66(11–12):1825–32.

[150] Huia J, Yuanyuan J, Jiao W, Yuan H, Yuan Z, Shiru J. Potentiality of bacterial cellulose as the scaffold of tissue engineering of cornea. The 2nd Conference on Biomedical Engineering and Informatics. China; 2009.

[151] Cai Z, Hou C, Yang G. Poly(3-hydroxubutyrateco-4-hydroxubutyrate)/bacterial cellulose composite porous scaffold: preparation, characterization and biocompatibility evaluation. Carbohydr Polym. 2012;87:1073–80.

[152] Phisalaphong M, Suwanmajo T, Tammarate P. Synthesis and characterization of bacterial cellulose/alginate blend membranes. J Appl Polym Sci. 2008;107(5):3419–24.

[153] Chiaoprakobkij N, Sanchavanakit N, Subbalekha K, Pavasant P, Phisalaphong M. Characterization and biocompatibility of bacterial cellulose/alginate composite sponges with human keratinocytes and gingival fibroblasts. Carbohydr Polym. 2011;853:548–53.

[154] Cai Z, Kim J. Bacterial cellulose/poly(ethylene glycol) composite: characterization and first evaluation of biocompatibility. Cellulose. 2010;17(1):83–91.

[155] Pértile R, Moreira S, Andrade F, Domingues L, Gama M. Bacterial cellulose modified using recombinant proteins to improve neuronal and mesenchymal cell adhesion. Biotechnol Prog. 2012;28:526–32.

[156] Wang J, Wan Y, Huang Y. Immobilisation of heparin on bacterial cellulose-chitosan nano-fibres surfaces via the cross-linking technique. IET Nanobiotechnol. 2012;6:52–7.

[157] Gao C, Wan Y, Lei X, Qu J, Yan T, Dai K. Polylysine coated bacterial cellulose nanofibers as novel templates for bone-like apatite deposition. Cellulose. 2011;18:1555–61.

[158] Karaaslan MA, Tshabalala MA, Yelle DJ, Buschle-Diller G. Nanoreinforced biocompatible hydrogels from wood hemicelluloses and cellulose whiskers. Carbohydr Polym. 2011;86(1):192–201.

[159] Saska S, Teixeira LN, de Oliveira PT, Minarelli Gaspar AM, Lima Ribeiro SJ, Messad-deq Y, Marchetto R. Bacterial cellulose-collagen nanocomposite for bone tissue engi-neering. J Mater Chem. 2012;22:22102–12.

[160] Wan Y, Gao C, Han M, Liang H, Ren K, Wang Y, Luo H. Preparation and characteri-zation of bacterial cellulose/heparin hydrib nanofiber for potential vascular tissue en-gineering scaffolds. Polym Adv Technol. 2011;22:2643–8.

[161] Wang M, Yuan J, Huang X, Cai X, Li L, Shen J. Grafting of carboxybetaine brush onto cellulose membranes via surface-initiated ARGET-ATRP for improving blood com-patibility. Colloids Surfaces B Biointerfaces [Internet]. 2013;103(0):52–8. Available from: http://www.sciencedirect.com/science/article/pii/S0927776512005826

[162] Solway DR, Clark WA, Levinson DJ. A parallel open–label trial to evaluate microbial cellulose wound dressing in the treatment of diabetic foot ulcers. Int Wound J. 2011;8(1):69–73.

[163] Portal O, Clark WA, Levinson DJ. Microbial cellulose wound dressing in the treat-ment of nonhealing lower extremity ulcers. Wounds. 2009;21(1):1–3.

[164] Wu, L.; Zhou, H.; Sun, H.-J.; Zhao, Y.; Yang, X.; Cheng, S. Z. D.; Yang, G. Thermores-ponsive bacterial cellulose whisker/poly(NIPAM-co-BMA) nanogel complexes: syn-thesis, characterization, and biological evaluation. Biomacromolecules. 2013;14:1078–84.

[165] Fernandes SCM, Sadocco P, Aonso-Varona A, Palomares T, Eceiza A, Silvestre AJD, Mondragon I, Freire CSR. Bioinspired antimicrobial and biocompatible bacterial cel-lulose membranes obtained by surface functionalization with aminoalkyl groups. ACS Appl Mater Interfaces. 2013;5:3290–7.

[166] Cassano R, Trombino S, Ferrarelli T, Nicoletta FP, Mauro MV, Giraldi C, Picci N. Hemp fiber (*Cannabis sativa* L.) derivatives with antibacterial and chelating proper-ties. Cellulose. 2013;20:547–57.

[167] Caldeira E, Piskin E, Granadeiro L, Silva F, Gouveia ICJ. Biofunctionalization of cel-lulosic fibres with L-cysteine: assessment of antibacterial properties and mechanism of action against *Staphylococcus aureus* and *Klebsiella pneumonia*. Biotechnol. 2013;168:426–35.

[168] Cassano R, Trombino S, Ferrarelli T, Barone E, Arena V, Mancuso C, Picci N. Synthe-sis, characterization, and anti-inflammatory activity of diclofenac-bound cotton fi-bers. Biomacromolecules. 2010;11:1716–20.

[169] Wei B, Yang GA, Hong F S. Preparation and evaluation of a kind of bacterial cellu-lose dry films with antibacterial properties. Carbohydr Polym. 2011;84(1):533–8.

[170] Sun X, Zhang L, Cao Z, Deng Y, Liu L, Fong H, Sun Y. Electrospun composite nano-fiber fabrics containing uniformly dispersed antimicrobial agents as an innovative

type of polymeric materials with superior antimicrobial efficacy. ACS Appl Mater Interfaces. 2010;2:952–6.

[171] Fortunati, E., Armentano, I., Zhou, Q., Iannoni, A., Saino, E., Visai, L. et al. Multifunctional bionanocomposite films of poly(lactic acid) cellulose nanocrystals and silver nanoparticles. Carbohydr Polym. 2012;87:1596–605.

[172] Dufresne A. Nanocellulose: a new ageless bionanomaterial. Mater Today. 2013;16(220–227):220–7.

[173] Song J, Tang A, Liu T, Wang J. Fast and continuous preparation of high polymerization degree cellulose nanofibrils and their three-dimensional macroporous scaffold fabrication. Nanoscale. 2013;5:2482–90.

[174] Baek C, Hanif Z, Cho SW, Kim DI, Um SH. Shape control of cellulose nanocrystals via compositional acid hydrolysis. J Biomed Nanotechnol. 2013;9(7):1293–8.

[175] Lahiji RR, Xu X, Reifenberger R, Raman A, Rudie A, Moon RJ. Atomic force microscopy characterization of cellulose nanocrystals. Langmuir. 2010;26(6):4480–8.

[176] Postek MT, Vladar A, Dagata J, Farkas N, Ming B, Sabo R, Wegner TH, Beecher J. Cellulose nanocrystals the next big nano-thing? Instrumentation, Metrology, and Standards for Nanomanufacturing II. Proceedings of SPIE—The International Society for Optical Engineering, San Diego, 2008;7042:1–11.

[177] Kolakovic R. Nanofibrillar Cellulose in Drug Delivery. University of Helsinki; 2013. p. 60.

[178] Cesca K, Cacicedo ML, Bossio VE, Castro GR, Porto LM. BaCarb™: a novel bioinorganic matrix for local drug delivery. BMC Proc. 2014;8:77.

[179] Kolakovic R, Laaksonen T, Peltonen L, Laukkanen A, Hirvonen J. Spray-dried nanofibrillar cellulose microparticles for sustained drug release. Int J Pharm. 2012;430(1–2):47–55.

[180] Trovatti E, Freire CSR, Pinto PC, Almeida IF, Costa P, Silvestre AJD, et al. Bacterial cellulose membranes applied in topical and transdermal delivery of lidocaine hydrochloride and ibuprofen: in vitro diffusion studies. Int J Pharm [Internet]. 2012;435(1): 83–7. Available from: http://www.sciencedirect.com/science/article/pii/ S0378517312000063

[181] Chang CW WM. Preparation of microfibrillated cellulose composites for sustained release of H_2O_2 or O_2 for biomedical applications. ACS Sustain Chem Eng. 2013;1:1129–34.

[182] Weng L, Rostamzadeh P, Nooryshokry N, Le HC, Golzarian J. In vitro and in vivo evaluation of biodegradable embolic microspheres with tunable anticancer drug release. Acta Biomater. 2013;9(6):6823–33.

[183] Ernsting MJ, Tang WL, MacCallum N, Li SD. Synthetic modification of carboxymethylcellulose and use thereof to prepare a nanoparticle forming conjugate of docetax-

el for enhanced cytotoxicity against cancer cells. Bioconjugate Chem. 2011;22:2474–86.

[184] Wen Y, Oh JK. Dual-stimuli reduction and acidic pH-responsive bionanogels: intracellular delivery nanocarriers with enhanced release. RSC Adv. 2014;4:229–37.

[185] Justin O. Zoppe, Ville Ruottinen, Janne Ruotsalainen, Seppo Rönkkö, Leena-Sisko Johansson, Ari Hinkkanen, Kristiina Järvinen, and Jukka Seppälä. Synthesis of cellulose nanocrystals carrying tyrosine sulfate mimetic ligands and inhibition of alphavirus infection. Biomacromolecules. 2014;15(4):1534–42.